Numerical Estimation of Extractable Wave Power around the Cylindrical Walled Breakwater

Radhakrishnan P. V.[1], Dr. Senthil Prakash M. N.[2], Dr. Satheesh Babu P.K.[3]

[1]*Research Scholar, Department of Ship Technology,*
Cochin University of Science & Technology, Kochi, Kerala, India.

[2]*Professor, Division of Mechanical Engineering,*
Cochin University of Science & Technology, Kochi, Kerala, India.

[3]*Associate professor, & Head of the Department, Department of Ship Technology,*
Cochin University of Science & Technology, Kochi, Kerala, India.

Abstract- Wave energy is a potent form of renewable energy. Considering the enormous potential of this form of energy, tapping this efficiently can significantly boost the renewable energy industry. In addition to being more predictable than solar or wind energy, wave energy has a higher energy density, ie more extractable energy per unit area. Since the need of fuels is increasing and the use of fossil fuels poses a threat in the form of global climate change, finding cleaner alternative energy sources has become the need of the hour. In order to protect inshore waters from waves and prevent coastal erosion, breakwaters are built on coasts as form of coastal defense mechanism. The breakwaters can also be used to offer secure harborage. Breakwater will produce a wave energy concentration close to its cylindrical wall. A dissipation of wave energy happens as it proceeds to the shore crossing the breaker and reaches the shore with a relatively lesser energy thus reducing the wave action on the shore resulting in a relatively calm sea close to the onshore. In order to extract wave energy effectively, breakwaters can be integrated with wave energy converters. The dual benefits of coastal protection and wave energy extraction are provided by breakwaters coupled with wave energy converters (WECs). An array of heaving-buoy WEC can be effectively utilized for this purpose. The objective of this work is to estimate the extractable wave power around the cylindrical walled breakwater numerically. The numerical estimation of extractable wave power is carried out by Computational Fluid Dynamics (CFD) technique. 3D incompressible Reynolds Averaged Navier-Stokes equation was the governing equation for the analysis. Volume of Fluid (VOF) approach with k–omega Shear Stress Transport (SST) viscous model was used for the CFD analysis. The numerical scheme of simulation was determined through an experimental validation of the numerical results with the experimental data extracted from the sector 1 near the cylindrical breakwater. The numerical results show that there is a considerable increase of wave height as the waves approach cylindrical wall of the breakwater.

Keywords –breakwater, wave energy converter, wave power, wave height, wave power density

I. INTRODUCTION

Air pollution and global climate change brought on by the continued use of fossil fuels has become a great concern for the lives on earth. Also fossil fuels, the main source of energy are getting depleted. Since the use of fossil fuels is increasing and posing a threat to global climate change, finding clean, alternative energy sources and is quickly emerging as the top priority of the century. Therefore the development and implementation of alternative energy sources is very important for the development of the world. The best choice to overcome the situation is ocean wave energy production. Considering the enormous potential of the resource, producing electric power through wave energy can significantly boost the renewable energy industry. In addition to being more predictable than solar or wind energy, wave energy also has a higher energy density, ie. more energy extraction from unit area. Among the different WEC technologies Breakwater integrated wave energy converters are the best choice to wave energy extraction and coastal protection. In order to protect inshore waters from waves and prevent coastal erosion, breakwaters are built on coasts as part of coastal defense. They can also be used to offer secure harborage. It will produce a wave energy concentration close to the breakwater zone and wave energy dissipation as the waves approaches the shore. It results in a relatively calm sea close to the onshore. In order to gather wave energy, breakwaters can be integrated with wave energy converters. The dual benefits of coastal protection and wave energy extraction are provided by breakwaters coupled with wave energy converters (WECs). An array of heaving-buoy WEC can be effectively utilized for this purpose.

In the cylindrical walled breakwater, a cylindrical shaped wall is attached to the end of the breakwater as shown in figure 1. Cylindrical wall is faced to open sea. The incoming waves strike on the cylindrical wall and the water body moves

upward much like a standing wave causing an oscillating motion. The rise of water column will be higher than the incoming wave height. Heaving-buoy wave energy converters can be placed around the cylindrical wall to extract the wave energy from the oscillating water column. The low backwash of a wave reflected off the wall that meets a new incoming wave to form the collapsing breaker. In this paper, the estimation of extractable wave power around a cylindrical walled breakwater is conducted numerically. The numerical estimation of extractable wave power is carried out by Computational Fluid Dynamics (CFD) method.

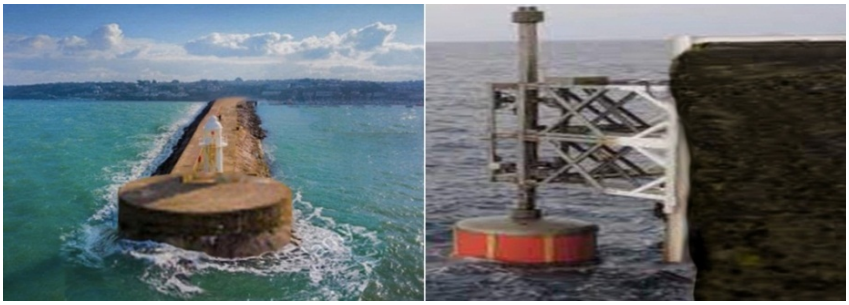

Figure 1. Cylindrical walled breakwater and heaving-buoy WEC attached to breakwater (source: https://commons.wikimedia.org)

II. ESTIMATION OF EXTRACTABLE WAVE POWERBY CFD METHOD

Numerical Estimation of Extractable Wave Power around the cylindrical walled breakwater was determined by Computational Fluid Dynamics simulation. 3D incompressible Reynolds Averaged Navier-Stokes equation was the governing equation for the CFD analysis. Volume of Fluid (VOF) approach with k–omega Shear Stress Transport (SST) viscous model was used. 3D representation of the body in the domain is shown figure 2. Length, width and height of the domain were 120 meter, 40 meter and 10 meter respectively. Dimensions of the body and domain are shown in figure 3.

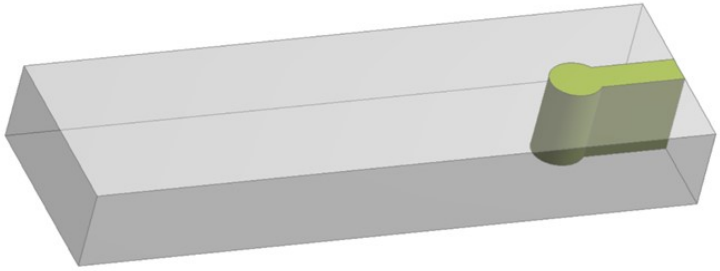

Figure 2. 3D representation of the body in the domain

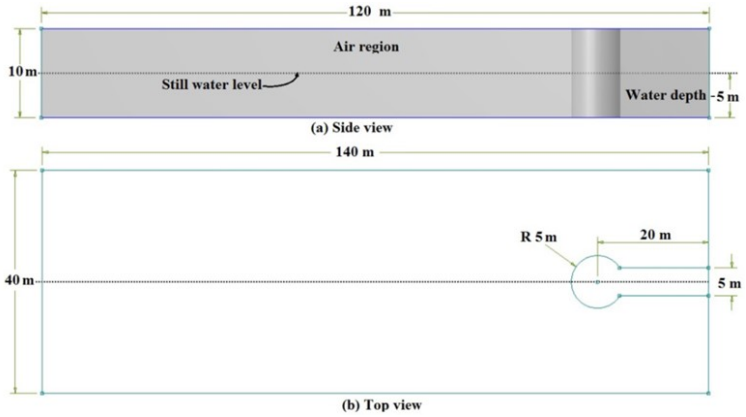

Figure 3. Dimensions of the body and domain

For the analysis, the fluid volume around the cylindrical wall is assumed to be divided into 30 sectors as shown figure 4. The radial width of the sectors is taken as 1 meter (condidering that heaving-buoy width is 1 meter) from the cylindrical wall. The sectors were sector 1, sector 1', sector 2, sector 2', sector 3, sector 3', sector 4, sector 4', sector 5, sector 5', sector 6, sector 6', sector 7, sector 7', sector 8, sector 8', sector 9, sector 9', sector 10, sector 10', sector 11, sector 11', sector 12, sector 12', sector 13, sector 13', sector 14, sector 14', sector 15, sector 15'. As the sectors, sector 1 and sector 1' to sector 15 and sector 15' are axisymmetric the wave power extracted will be approximately equal.

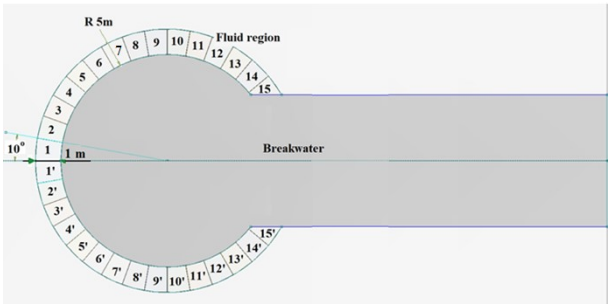

Figure 4. Pictorial representation of the sectors of fluid region

2.1Boundary conditions –

Transient simulation was conducted. The wave simulation was done applying open channel wave boundary condition. Boundary conditions for the analyses were as follows. Water depth was 5 m, incident wave height was 1 m, wave length was 25 m and wave period was 4.72 sec. Wave type was intermediate water wave. Stocks second order wave theory was selected for the analysis. The length, width, and height of the domain were 140 meters, 40 meters and 10 meters respectively.

III.RESULT AND DISCUSSIONS

3.1 Experimental set-up –

The experiment regarding the estimation of extractable wave power around the cylindrical walled breakwater was conducted in a wave basin. The length, width and depth of the wave basin are 12 m, 4 m and 0.5m respectively. The wave basin is equipped with a flap-type regular wave generator at one end and a wave-damper at the other end. The instantaneous readings from the sensors are collected to a computer system using a data logger. Schematic of experimental setup is shown in figure 5.

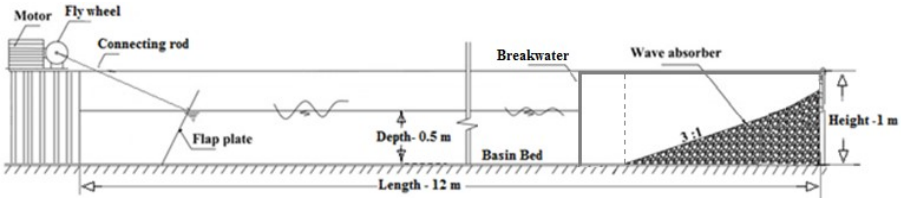

Figure 5. Schematic of experimental setup

3.2 Validation–

Froude similarity law is used for the experimental test of the scaled model. Scale ratio is taken as 10:1. Water depth, incident wave height, wave length and wave period were taken as 0.5m, 0.1 m, 2.5 m and 1.493 sec respectively. The Model dimensions are as shown in figure 6.

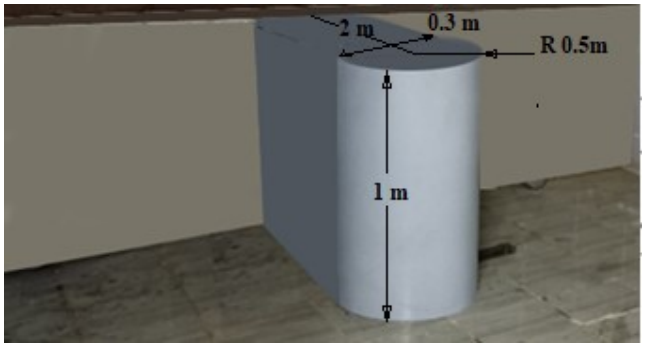

Figure 6. Experimental Setup - Cylindrical walled breakwater model in the wave tank.

The infrared sensor is placed in front of the cylindrical walled breakwater model, the scaled region corresponding to sector 1 of the numerical analysis. The instantanous readings of wave height from the sensor is collected using the data logger. The experiment was cunducted for 60 seconds. Three sets of readings were collected and the average was used for the validation. The validation was carried out by compairing the experimental data with the numerical data.

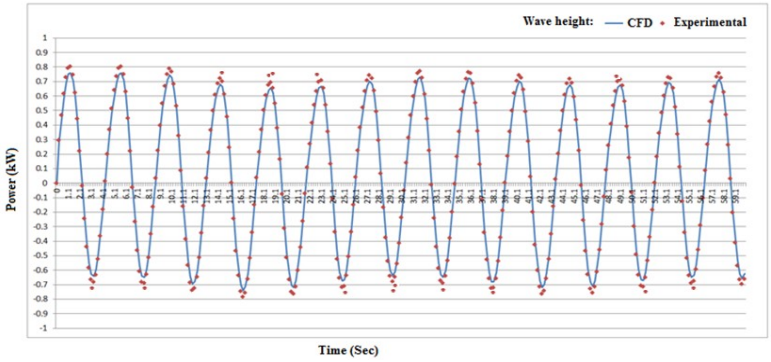

Figure 7. Experimental validation of Numerical result.Temporal history of wave height.

3.3 Extractablewave power atsector 1 and sector 1'–

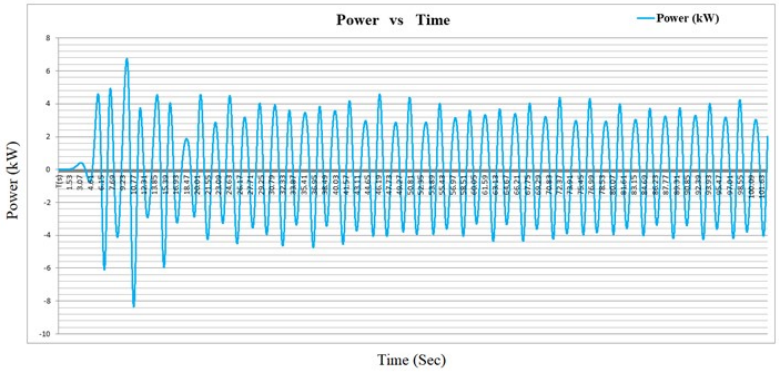

Figure 8. Time series for wave power at sector 1 and sector 1' (Numerical)

The extractable average wave power at sector 1 and 1' was 2.345 kW. The power per unit water surface area (power density) at sector 1 and 1' calculated through the simulation was 2.154 kW/m^2. Maximum power was obtained from these sectors.

3.4Extractablewave power atsector 2 and sector 2'–

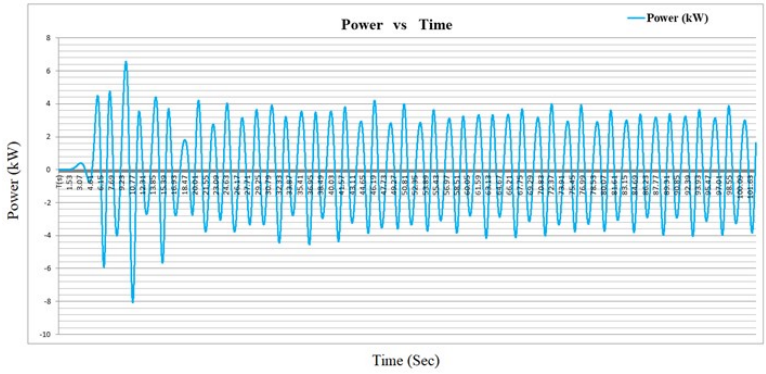

Figure 9. Time series for wave power at sector 2 and sector 2'(Numerical)

The extractable average wave power at sector 2 and 2' was 2.185 kW. The power density was 2.007 kW/m^2. The average extractable wave power calculated at this sectors is lower than that at sectors 1 and 1'.

3.5Extractablewave power atsector 3 and sector 3'–

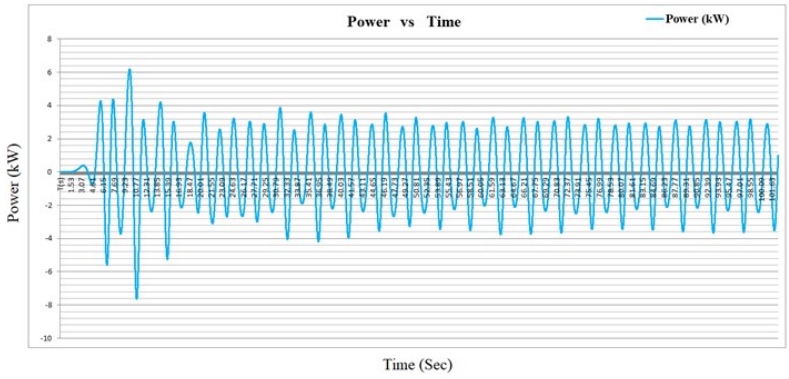

Figure 10. Time series for wave power at sector 3 and sector 3'(Numerical)

The extractable average wave power at sector 3 and 3' was 1.906 kW. The power density was 1.75 kW/m^2. The average extractable wave power calculated at this sectors is lower than that at sectors 2 and 2'.

3.6 Extractablewave power atsector 4 and sector 4'–

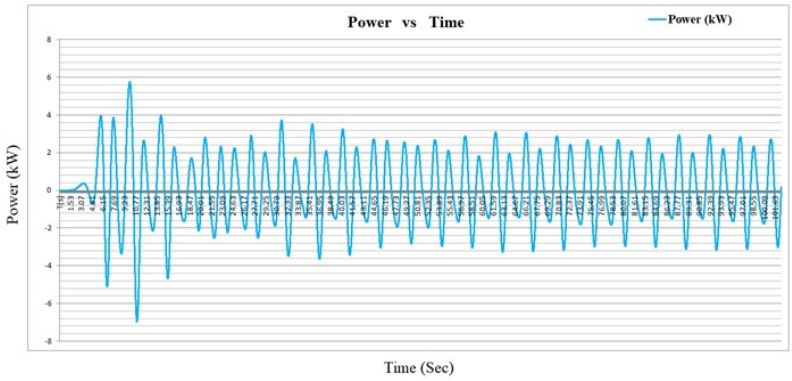

Figure 11. Time series for wave power at sector 4 and sector 4'(Numerical)

The extractable average wave power at sector 4 and 4' was 1.571 kW. The power density was 1.442 kW/m^2. The average extractable wave power calculated at this sectors is lower than that at sectors 3 and 3'.

3.7 Extractablewave power atsector 5 and sector 5'–

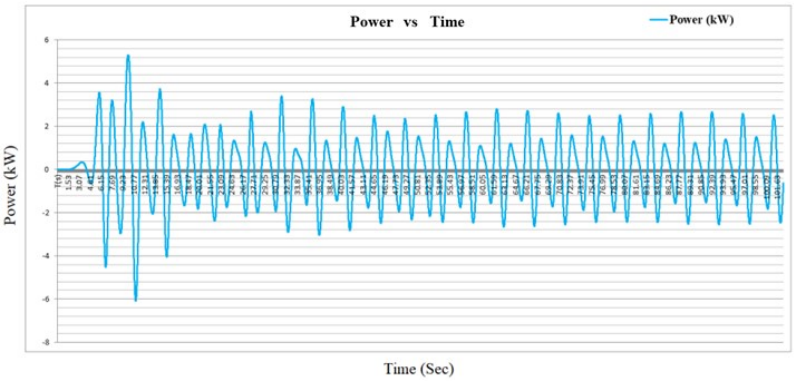

Figure 12. Time series for wave power at sector 5 and sector 5'(Numerical)

The extractable average wave power at sector 5 and 5' was 1.297 kW. The power density was 1.191 kW/m^2. The average extractable wave power calculated at this sectors is lower than that at sectors 4 and 4'.

3.8 Extractablewave power atsector 6 and sector 6'–

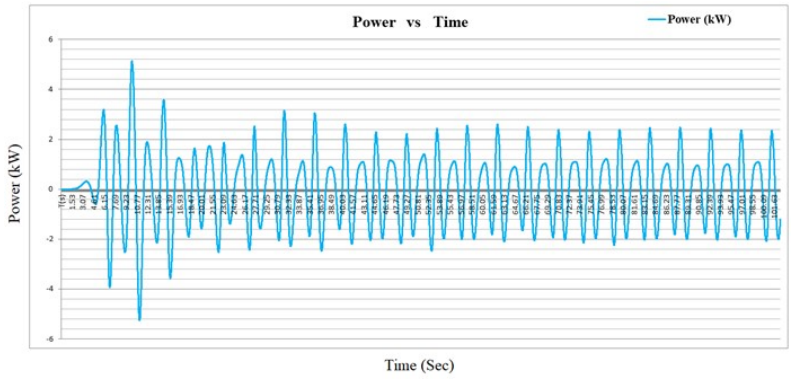

Figure 13. Time series for wave power at sector 6 and sector 6'(Numerical)

The extractable average wave power at sector 6 and 6' was 1.198 kW. The power density was 1.101 kW/m^2. The average extractable wave power calculated at this sectors is lower than that at sectors 5 and 5'.

3.9 Extractablewave power atsector 7 and sector 7'–

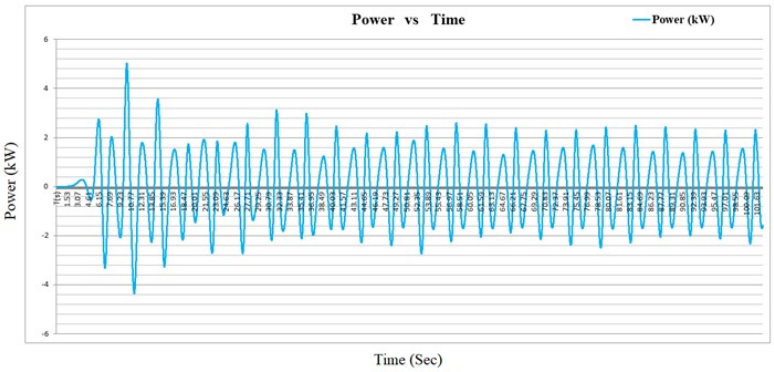

Figure 14. Time series for wave power at sector 7 and sector 7'(Numerical)

The extractable averagewave power at sector 7 and 7' was 1.194kW. The power density was 1.097 kW/m^2. The average extractable wave power calculated at this sectors is lower than that at sectors 6 and 6'.

3.10 Extractablewave power atsector 8 and sector 8'–

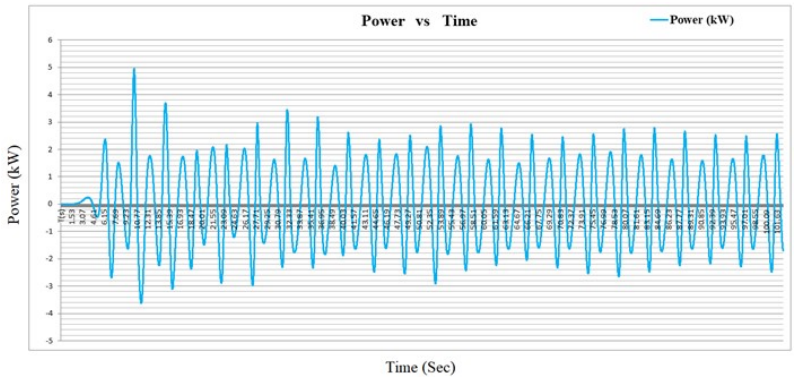

Figure 15. Time series for wave power at sector 8 and sector 8'(Numerical)

The extractable average wave power at sector 8 and 8' was 1.262 kW. The power density was 1.159 kW/m^2. The average extractable wave power calculated at this sectors is higher than that at sectors 7 and 7'.

3.11 Extractablewave power atsector 9 and sector 9'–

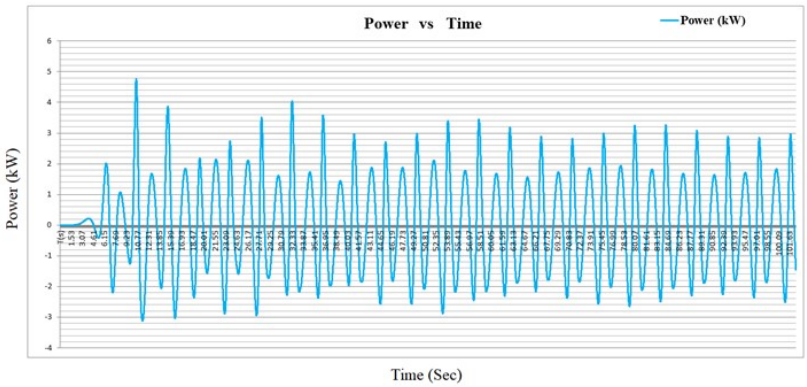

Figure 16. Time series for wave power at sector 9 and sector 9'(Numerical)

The extractable average wave power at sector 9 and 9’ was 1.338 kW. The power density was 1.229 kW/m^2. The average extractable wave power calculated at this sectors is higher than that at sectors 8 and 8’.

3.12 Extractablewave power atsector 10 and sector 10’–

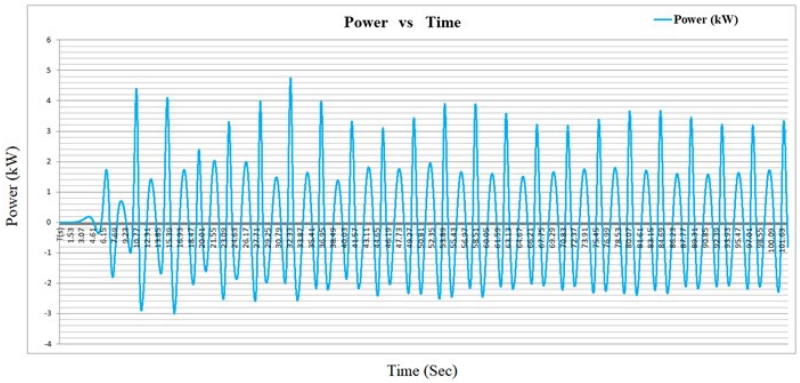

Figure 17. Time series for wave power at sector 10 and sector 10’(Numerical)

The extractable average wave power at sector 10 and 10’ was 1.347 kW. The power density was 1.237 kW/m^2. The average extractable wave power calculated at this sectors is higher than that at sectors 9 and 9’.

3.13 Extractablewave power atsector 11 and sector 11’–

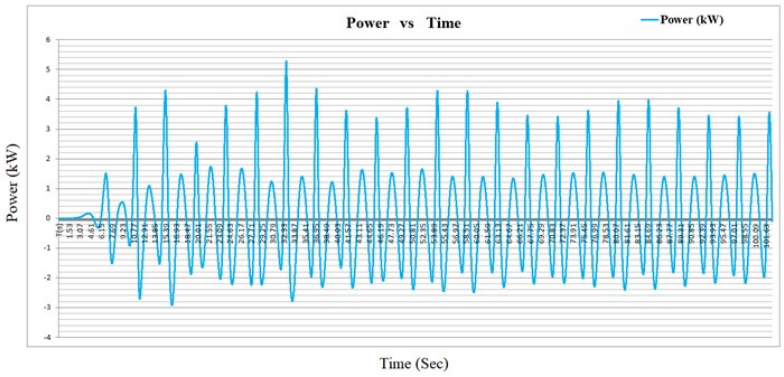

Figure 18. Time series for wave power at sector 11 and sector 11’(Numerical)

The extractable average wave power at sector 11 and 11’ was 1.286 kW. The power density was 1.181 kW/m^2. The average extractable wave power calculated at this sectors is lower than that at sectors 10 and 10’.

3.14 Extractablewave power atsector 12 and sector 12’–

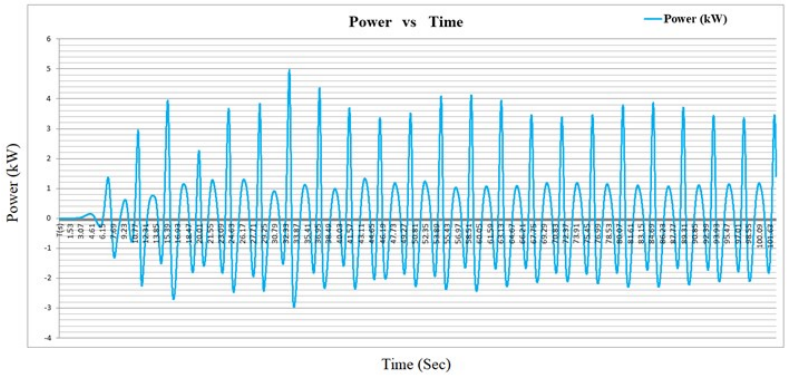

Figure 19. Time series for wave power at sector 12 and sector 12'(Numerical)

The extractable average wave power at sector 12 and 12' was 1.181 kW. The power density was 1.084 kW/m^2. The average extractable wave power calculated at this sectors is lower than that at sectors 11 and 11'.

3.15 Extractable wave power atsector 13 and sector 13'–

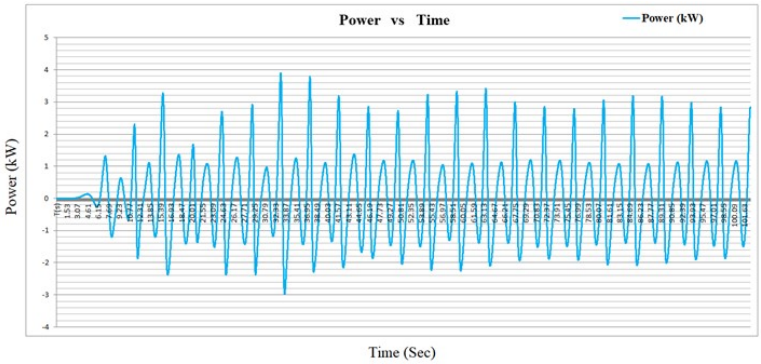

Figure 20. Time series for wave power at sector 13 and sector 13'(Numerical)

The extractable average wave power at sector 13 and 13' was 1.027 kW. The power density was 0.943 kW/m^2. The average extractable wave power calculated at this sectors is lower than that at sectors 12 and 12'.

3.16 Extractable wave power atsector 14 and sector 14'–

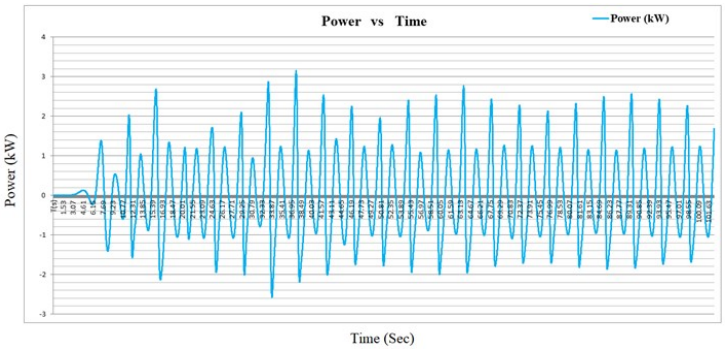

Figure 21. Time series for wave power at sector 14 and sector 14'(Numerical)

The extractable average wave power at sector 14 and 14' was 0.876 kW. The power density was 0.805 kW/m^2. The average extractable wave power calculated at this sectors is lower than that at sectors 13 and 13'.

3.17 Extractable wave power atsector 15 and sector 15'–

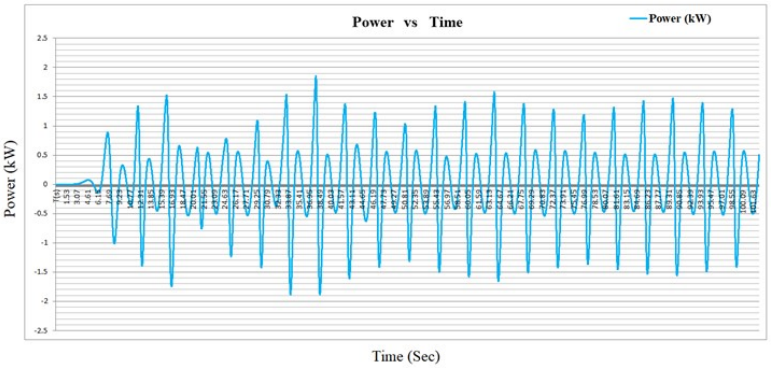

Figure 22. Time series for wave power at sector 15 and sector 15'(Numerical)

The extractable average wave power at sector 15 and 15' was 0.509 kW. The power density was 0.468 kW/m^2. The average extractable wave power calculated at this sectors is lower than that at sectors 14 and 14'.

Sectors	1 & 1'	2 & 2'	3 & 3'	4 & 4'	5 & 5'	6 & 6'	7 & 7'	8 & 8'	9 & 9'	10 & 10'	11&11'	12&12'	13&13'	14&14'	15&15'
Average Power (kW)	2.345	2.185	1.906	1.571	1.297	1.198	1.194	1.262	1.338	1.347	1.286	1.181	1.027	0.876	0.509
Power density (kw/m^2)	2.154	2.007	1.751	1.443	1.191	1.101	1.097	1.159	1.229	1.237	1.181	1.084	0.943	0.805	0.468

Table 1. Estimated extractable average wave power and power density at different sectors (Numerical)

IV. CONCLUSION

3D Computational Fluid Dinamics simulations of wave effect on cylindrical walled breakwater to calculate the extractable wave power arround the breakwater is described. The validation of the scheme of numerical analysis is done by contrasting the relative wave height obtained from experimental analysis with that derived from CFD analysis for one sector and a reasonable agreement is obtained. The results show a wave height amplification up to 1.5 times while using cylinderical walled wave breaker. The maximum extractable wave power was found available near sectors 1 and 1'.It is observed that wave power is minimum at sectors 15 and 15'. The reduction in exttractable wave power is due to wave damping. The analysis reveals that the cylindrical walled breakwaters can create wave energy hot spots over specific portion around it. Wave energy extractors can be placed in this region for efficient and economical extraction of energy.

REFERENCES

[1] B. Corona, M. Nakano, H. Pérez, "Adaptive Watermarking Algorithm for Binary Image Watermarks", *Lecture Notes in Computer Science,Springer, pp. 207-215, 2004.*

[2] Umesh A. Korde and Cengiz Ertekin R, "On wave energy focusing and conversion in open water", *Renewable Energy, Vol.62, pp. 84-99, 2014.*

[3] Veigas M, Lopez M and Iglesias G, "Assessing the optimal location for a shoreline wave energy converter", *Applied Energy, Vol. 132, pp. 404–411, August 2014.*

[4] Venkatesan R, Vengatesan G, Vedachalam N, Arul Muthiah M, Lavanya R and Atmanand M.A, "Reliability assessment and integritymanagement of data buoy instruments used for monitoring the Indian Seas", *Applied Ocean Research, Vol. 54, pp. 1–11, 2016.*

[5] Vivek kumar Gope, Ankit Aggarwal, Shivaraj S.M and Arkal Vittal Hegde, "Simulation using Computational fluid Dynamics (CFD) forSemi-Circular Breakwater during flow over it", *International Journal of Scientific & Engineering Research, Vol. 7, Issue. 7, pp. 396-401, ISSN: 2229-5518, July 2016.*

[6] Wassim Chehazea, Dory Chamoun, Charbel Bou-Mosleh and Pierre Rahme, "Wave Roller Device for Power Generation", *Procedia Engineering, Vol. 145, pp. 144 – 150, 2016.*

[7] YanjiWei, Thomas Abadie, AlanHenry and Frederic Dias, "Wave interaction with an Oscillating Wave Surge Converter. PartII:Slamming", *Ocean Engineering, Vol.113, pp. 319–334, 2016.*

[8] Yongyao Luo, Jean-Roch Nader, Paul Cooper and Song-Ping Zhu, "Nonlinear 2D analysis of the efficiency of fixed Oscillating WaterColumn wave energy converters", *Renewable Energy, Vol. 64, pp. 255-265, 2014.*

[9] Zhao Chen, Chen Zezong, Jiang Yanni, Fan Lingang and Zeng Gengfei, "Exploration and Validation of Wave-Height Measurement UsingMultifrequency HF Radar", *Journal of Atmospheric and Oceanic Technology, Vol. 30, pp. 2189-2202, September 2013.*

[10] Zivko Kokolanski, Josep Jordana, Manel Gasulla, Vladimir Dimcev and Ferran Reverter, "Direct inductive sensor-to-microcontrollerinterface circuit", *Sensors and Actuators, A xxx, pp. 0924-4247, January 2015.*